We are IntechOpen,
the world's leading publisher of
Open Access books
Built by scientists, for scientists

6,900
Open access books available

186,000
International authors and editors

200M
Downloads

Our authors are among the

154
Countries delivered to

TOP 1%
most cited scientists

12.2%
Contributors from top 500 universities

CLARIVATE ANALYTICS
BOOK CITATION INDEX
INDEXED

WEB OF SCIENCE™

Selection of our books indexed in the Book Citation Index
in Web of Science™ Core Collection (BKCI)

Interested in publishing with us?
Contact book.department@intechopen.com

Numbers displayed above are based on latest data collected.
For more information visit www.intechopen.com

2

Numerical Simulation on the Steady and Unsteady Internal Flows of a Centrifugal Pump

Wu Yulin, Liu Shuhong and Shao Jie
Tsinghua University
China

1. Introduction

Nowadays, pumps of different size are needed for a great variety of purposes. In the past, both computational fluid dynamics (CFD) and experimental flow visualization were performed to reveal flow characteristics within centrifugal pumps, to examine a specific design and to guide design improvement (see Burgreen et al. 1996, 2000). Li et al. (2007) studied the interior viscous flow in a mini pump with an asymmetric axis using CFD and PIV (particle image velocimetry) for improvement of the pump design. Matsui et al. (2002) adopted the the k-ω model in the CFD simulation for a centrfugal pump, and the computational grid system only consisted of one flow passage for LDV (laser Dopler velocimetry) test impeller.

Byskov et al. (2003a) and Pedersen & Larsen (2003 b) investigated the flow inside the rotating passages of a six-bladed shrouded centrifugal pump impeller using LES simulation and PIV and LDV measurements. The velocities predicted with LES were in good agreement with the experimental data. The two RANS simulations were, however, not able to predict this complex flow field. It was thus found that using LES for analyzing the flow field in centrifugal pumps could shed light on basic fluid dynamic with a satisfactory accuracy compared to experiments.

A transient simulation was used to study the effects of pulsatile blood flow due to the heartbeat through blood pumps by Song et al. (2003). The microsized geometry of the pump made the choice of turbulence models significant for the accuracy of calculation. The comparison showed that the k-ω model gave better predictions of the shear level within the near wall regions than the k-ε model. Guleren and Pinarbasi (2004) indicated that the stallcell size extended from one to two diffuser passages. Comparisons of the computational results with experimental data were made and showed good agreement.

The unsteady flow in a low specific speed radial diffuser was simulated by the CFD code CFX-10 by Feng et al. (2009). The PIV and LDV measurements had been conducted to validate the CFD results. Both the phase-averaged velocity fields and the turbulence fields obtained from different methods are presented and compared.

In this study, in order to get more information about the internal flow of a centrifugal pump, both experimental measurement and numerical simulation are engaged. A centrifugal model pump test rig is built for PIV measurement. The test, involving the technology of index match and fluorescent, is for acquiring flow pattern in a fixed rotational speed, the velocity distribution of the flow field are thus obtained. And, the RANS (Reynolds

Averaged Navier-Stokes) tubulent equations with the SST k-ω turbulence model are applied to simulate its 3D steady whole passage flow and the DES (Dettached Eddy Simulation) method to simulate this unsteady flow. The external characteristics and the internal flow pattern of the centrifugal pump are calculated. According to comparison with experimental data, the unsteady simulation is proved to be relatively accurate in predicting the flow status in the centrifugal model pump.

2. Numerical simulation

The three-dimensional geometry model of the mini pump is generated using a 3D modeling software package (Gambit, v2.2.60, Fluent Inc., Lebanon, NH, USA). The computational domains include the inlet, outlet, impeller and the volute. Then the geometry is meshed in 3D Tet/Hybrid elements.

An unstructured-mesh finite-volume-based commercial CFD package, Fluent (v6.2.16, Fluent Inc.), is used to solve the incompressible steady Naiver-Stokes equations.

The incompressible continuity equation and Reynolds averaged the N-S equations are employed to simulate the steady turbulent flow through the pump, and the SST k-ω double equation turbulence model is adopted to make the equations closed.

2.1 Turbulence model

The k-ω based Shear-Stress-Transport (SST) model is designed to give highly accurate predictions of the onset and the amount of flow separation under adverse pressure gradients, because it takes transport effects into the formulation of the eddy-viscosity. This resulted in a major improvement in terms of flow separation predictions by Menter (1994).

In the SST k−ω turbulence model, the turbulent kinetic energy k equation is used. But the turbulent dissipation rate equation in k−ε is replaced by the turbulent dissipation frequency ω,

$$\omega = \frac{\varepsilon}{C_k k} \tag{1}$$

And k and ω equations are as follows:

$$\frac{\partial}{\partial t}(\rho k) + \frac{\partial}{\partial x_j}(\rho k \bar{u}_j) = \frac{\partial}{\partial x_j}\left(\Gamma_k \frac{\partial k}{\partial x_j}\right) + P_k - Y_k \tag{2}$$

$$\frac{\partial}{\partial t}(\rho \omega) + \frac{\partial}{\partial x_j}(\rho \omega \bar{u}_j) = \frac{\partial}{\partial x_j}\left(\Gamma_\omega \frac{\partial \omega}{\partial x_j}\right) + P_\omega - Y_\omega + D_\omega \tag{3}$$

where P_k is the productive term of k, P_ω the productive term of ω, Γ_k and Γ_ω are the diffusion coefficients of k and ω, Y_k and Y_ω the disspation terms of k and ω respectively, and D_ω is the orthogonal diffusion term. The productive terms are as follows:

$$P_k = -\rho \overline{u_i' u_j'} \frac{\partial \bar{u}_j}{\partial x_i}, \ P_\omega = \frac{\alpha_\infty}{\nu_t} P_k,$$

where $\alpha_\infty = F_1 \alpha_{\infty,1} + (1-F_1)\alpha_{\infty,2}$, $\alpha_{\infty,1} = \dfrac{\beta_{i,1}}{\beta_\infty^*} - \dfrac{\kappa^2}{\sigma_{\omega,1}\sqrt{\beta_\infty^*}}$, $\alpha_{\infty,2} = \dfrac{\beta_{i,2}}{\beta_\infty^*} - \dfrac{\kappa^2}{\sigma_{\omega,2}\sqrt{\beta_\infty^*}}$, and

$F_1 = \tanh\left(\arg_1^4\right)$ ($\arg_1 = \max\left(\min\left(\dfrac{\sqrt{k}}{0.09\omega y}, 0.45\dfrac{\omega}{\Omega}\right), \dfrac{400\mu}{\rho l^2 \omega}\right)$, l is the distance to next surface).

The diffusion coefficients are

$$\Gamma_k = \mu + \frac{\mu_t}{\sigma_k}, \quad \Gamma_\omega = \mu + \frac{\mu_t}{\sigma_\omega}$$

where σ_k and σ_ω are the Prandtle numbers of k and ω , and the eddy viscosity is:

$$\mu_t = \left(\frac{\rho k}{\omega}\right) \bigg/ \max\left[\frac{1}{\alpha^*}, \frac{\overline{\Omega}F_2}{\alpha_1 \omega}\right] \tag{4}$$

where $\alpha^* = \alpha_\infty^*\left(\dfrac{\alpha_0^* + \mathrm{Re}_t/R_k}{1 + \mathrm{Re}_t/R_k}\right)$, $\overline{\Omega} \equiv \sqrt{\overline{\Omega_{ij}}\,\overline{\Omega_{ij}}}$, $\sigma_k = \dfrac{1}{F_1/\sigma_{k,1} + (1-F_1/\sigma_{k,2})}$,

$\sigma_\omega = \dfrac{1}{F_1/\sigma_{\omega,1} + (1-F_1/\sigma_{\omega,2})}$, $F_2 = \tanh\left(\arg_2^2\right)$ $\left(\arg_2 = \max\left(2\dfrac{\sqrt{k}}{0.09\omega y}, \dfrac{400\mu}{\rho y^2 \omega}\right)\right)$, where $\overline{\Omega}_{ij}$ is vorticity.

The disspation terms Y_k , Y_ω and D_ω are as follows:

$$Y_k = \rho\beta_\infty^* k\omega, \quad Y_\omega = \rho\beta_\infty^* \omega^2, \quad D_\omega = 2(1-F_1)\rho\sigma_{\omega,2}\frac{1}{\omega}\frac{\partial k}{\partial x_j}\frac{\partial \omega}{\partial x_j}$$

The constants in this model are $\sigma_{k1} = 0.85$, $\sigma_{\omega 1} = 0.65$, $\sigma_{k2} = 1.0$, $\sigma_{\omega,2} = 0.856$, $\kappa = 0.42$, $\beta_{i,1} = 0.075$, $\beta_{i,2} = 0.0828$, $\alpha_\infty^* = 1$, $\beta_\infty^* = 0.09$.

2.2 DES simulation based on SST k-ω model

The DES method is adapted to simulate the unsteady turbulent flow through the whole flow passage of the centrifugal pump. In DES method, the RANS turbulent flow simulation with the SST k-ω turbulence model is applied to simulate the boundary layer flow near solid walls and the LES simulation with the Smagorinski SGS (Subgrid Stress) model is used to simulate the flow in other regions.

The turbulence length $l_{k-\omega}$ of the SST k-ω model can be defined as

$$l_{k-\omega} = \sqrt{k} / (\beta_\infty^* \omega) \tag{5}$$

In DES simulation, the length $l_{k-\omega}$ will be replaced by the following expression:

$$\bar{l} = \min(l_{k-\omega}, C_{DES}\Delta) \tag{6}$$

where $\Delta = \max(\Delta x, \Delta y, \Delta z)$ is the maximum distance between two adjacent grid nodes. When $l_{k-\omega} < \Delta$, the RANS simulation with SST k-ω model is used, and when $l_{k-\omega} > \Delta$, the

LES is adopted for simulation of the turbulent flow. If the grid sizes are fine enough in whole computational region, the LES will be applied in the entire domain. The DES method is used in unstructured grid system in the present work. Near solid walls in the grid system where the value of ω is very large, k still remains the finite value, and $l_{k-\omega}$ is smaller than $\Delta = \max(\Delta x, \Delta y, \Delta z)$. Therefore RANS simulation with SST k-ω model is suitable for turbulent flow computation near walls as described by Mitchell et al. (2006) and C_{DES} = 0.65 for unstructured grid system.

3. Computational model of the centrifugal pump

3.1 Pump model and geometry

The pump and its impeller under investigation are centrifugal type shown in Fig. 1. The impller consists of six two-dimensioned curvature backward swept blades of constant thickness with arc profile leading edges and blunt trailing edges. Axial height of the impeller blade is tapered linearly from 15.13 mm at the inlet to 8.11 mm at the outlet. The entire impeller is manufactured in acryl for the PIV measurements at impeller passages. Table 1 summarizes the main dimensions of the test impeller. The computational domain includes the inlet, impeller, volute and oulet shown in Fig. 1.
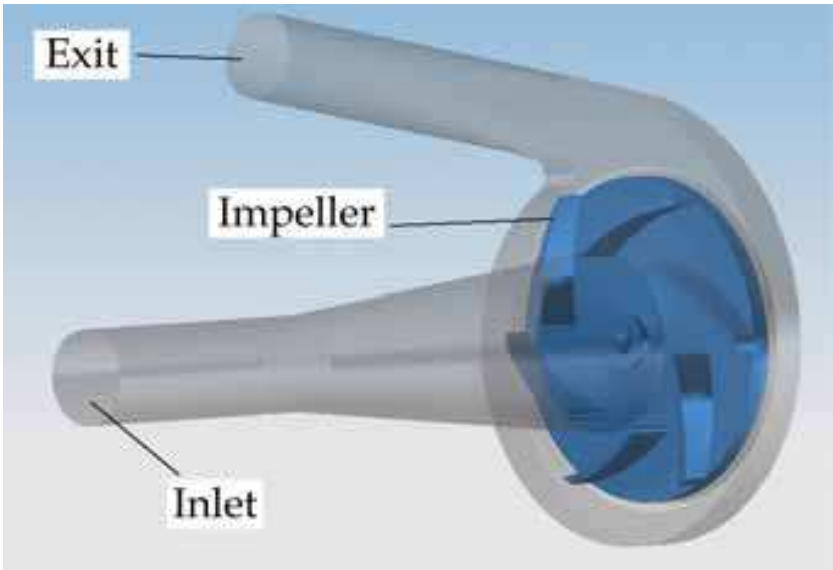

Fig. 1. The centrifugal pump

Geometry	Symbol	Value	Unit
Inlet diameter	D_1	55.14	mm
Outlet diameter	D_2	100	mm
Inlet height	b_1	15.13	mm
Outlet height	b_2	8.11	mm
Number of blades	Z	6	–
Blade thickness	t	2.7	mm
Inlet blade angle	β_1	15	deg.
Outlet blade angle	β_2	39	deg.

Table 1. Impeller geometry

3.2 Grid system independency verification

It is necessary to carry out independancy verification of the grid system before CFD computation. The varified case of the pump is design flow rate case with rotating speed of 1000rpm, flow rate of 46.65L/min and the design head of 1.36m (test result is 1.39m). 6 different grid systems are formed in the computational domain to perform this independy verification as drawn in Fig. 2.

Fig. 2 shows head variation with grid number of pump grid system at design flow rate case for grid number independency verification. According to it, once the total grid number of pump system is larger than 2,150,000, its calculated head will not change apparently. So the grid number for its steady and unsteady flow computation is selected as 2,150,000.
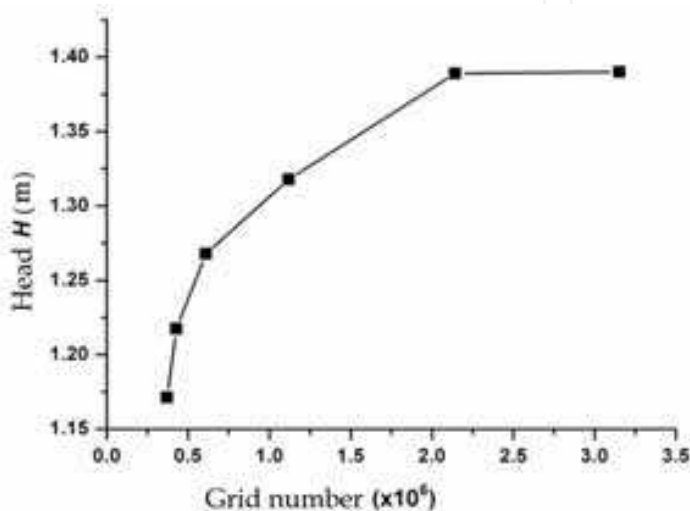
Fig. 2. Head variation with grid number of pump grid system at design flow rate case

3.3 Time step independancy verification for unsteady flow computation

It is necessary to carry out independancy verification of the time step before unsteady CFD computation. Tested case of the pump is also the design flow rate case. 6 different time steps are selected for the unsteady computation to perform this independy verification as listed in Table 2. The calculated pump heads in Table 2 are obtained after the unsteady computation. If the time step in computation is less than 0.0006 second, the pump head from unsteady flow computations will not change. So the time step is selected as 0.0006 for both calculation accuracy and ecomomic time consumption.

Time step（s）	0.03	0.006	0.002	0.001	0.0006	0.0002
Iteration steps	1000	1000	1000	1000	1000	1000
Calculated head (m)	No covergence	1.2907	1.3312	1.3681	1.4007	1.3971

Table 2. Calculated head for different time steps of unsteady flow simulation

3.4 Numerical simulation methods

Steady numerical simulation method

For the steady turbulent flow simulation in the centrifugal pump, the pump impeller is frozen in a definite position and the multiple reference frame is selected. The whole flow

passage of the pump includes spiral volute, inlet suction and impeller computed sub-domains. The impeller region is in the rotating reference frame, and other regions are in the stationary reference frame. The continuity of velocity vectors should be kept on the interface between two reference frames.

An unstructured-mesh finite-volume-based commercial CFD package, Fluent (v6.2.16, Fluent Inc.), is adopted to discretize governing equations of the flow computation. The variables are saved up at the center of a control volume. The SIMPLEC algorithm is applied for decoupling velocity and pressure solution. The second order central differencing scheme is adopted for the diffusive term, and the second order upwind differencing scheme for the convective terms. Calculated fluid is the refractive index solution for the pump test with density of 1050kg/m³ and viscosity of 0.0035kg/m-s.

The boundary conditions of the steady flow computation in the pump are set as follows:

a.   A mass-flow boundary condition is specified at the inle. The Dericlidt condition of each variable is given at the inlet of computational domain. For example, the velocity at inlet section is given according to the flow rate of the case and it was perpendicalar to the inlet section.

b.   An outflow condition is set at the outlet. The Neumann conditions is given for each variable.

c.   The wall function is adopted near the fixed wall, and non-slip boundary condition is adopted on the stationary wall. If the boundary is rotary, the velocity on the boundary wall is set as Ωr (where r is radius; Ω is the rotating speed of impeller) .

d.   For the pressure condition, Neumann conditions are specified on all boudaries, except for the pressure at one point. This point pressure would be specified as a reference value and it remains the same at each iteration. Then pressures at all stations are recalculated according to the reference value after each iteration.

Unsteady numerical simulation method

The DES turbulent computation is adopted for the unsteady flow in the centrifugal pump with SST k-ω turbulence model in this work. In the computation, the sliding meshes are formed between its stationary components and rotating ones in order to model the rotor-stator interactions between inlet and runner, and runner and volute. Based on the sliding mesh modeling, the unsteady characters of the pump could be obtained with the second order implicit time advancing scheme. The time step value had been verified and adopted as above. Then at each time step the same disctrete numerical treatment and boundary conditions are utilizied as those in steady flow simulation to capture the convergent instantaneous flow situation after the discretizing equations being solved. In the next step, with sliding meshes' moving to new position, the new position simulation would be carried out according to last time results and the second order implicit time advancing scheme.

4. Instantaneous PIV measurement on internal flows of the centrifugal pump

PIV is a technique which measures the instantaneous velocity field within an illuminated plane of fluid field by using light scattered from particles seeded into the fluid. PIV has recently matured to a reliable technique that is used in a wide variety of applications (Wu et al. 2009). The PIV hardware for this research consists of a 120mJ/pulse dual-cavity pulsed Nd: YAG laser, laser light sheet optics, a charge coupled device (CCD) camera, a synchronizer and a date's process system.

In order to eliminate the effect of refraction/reflection light from the area close to the walls and enhance the measurement accuracy, fluorescent particles are scattered into the working fluid with the tracing particles. The refractive index of water in pump and of the transparent material of pump impeller and volute with curved walls is different (Budwig, 1994). The beams of rays with different angles of incidence can not focus at a definite point, which will result in imaging defocused and deformed, and that leads to an error in the PIV measurement. The refractive index matched (RIM) fluid with the same refractive index as the transparent material has been prepared and applied in the present test of pump with geometrical complex walls to eliminate this type of error of PIV measurement.

The present PIV measurement with both the laser induced fluorescence (LIF) particles and the refractive index matched (RIM) facilities in the centrifugal pump is carried out and gives a reliable flow patterns in the pump. It is obvious that the application of LIF particle and RIM are the key methods to get good PIV measurement results in pump internal flow (see Wu et al. 2009).

4.1 Absolute velocity distribution and streamlines in impeller at design flow rate

Fig. 3 (a) shows the mean absolute velocity distribution and streamlines of the PIV measurement in impeller under design flow rate condition at the moment of t=0 (see Fig. 4 (a)). The absolute streamlines in the pump are distributed smoothly; the absolute mean velocity magnitude varies from the value less than 1 m/s at the impeller inlet area to more 4 m/s at the outlet of impeller. And near the impeller outlet, the absolute velocity near suction surfaces of blades is larger than that near pressure surfaces.

Fig. 3 (a) shows the distributions of sampling points in the measuring plan of the pump, where point 1 is in the impeller passage and point 2 in the outlet area. Fig. 3 (b) shows measuring uncertainty at design flow rate condition with respective to times of measurement. From this figure, it can be observed that if the time of measurement is larger than 200, the uncertainty of measuring velocity is less than ±0.03m / s which means the error of this velocity measurement is less than ± 4%.

4.2 Relative velocity distribution and streamlines in impeller at design flow rate

Fig. 4 shows the relative velocity and streamlines distribution in impeller at design flow rate condition (Q=Q_d= 2.70m³/s) from this PIV measurement. In Fig. 4, there are 5 pictures (a) to (e) to display the velocity for different position of impeller vanes. The time interval between two positions is one fifth of the period T of impeller rotation. The flow distributions on 5 pictures are almost the same which illustrates the impeller manufactured axisymmetrically and also the measurement with reliability. The flow difference in different blade channels occurs near the tongue, which affects the flow in the channel greatly.

At the design flow rate condition, the relative velocity in the blade channel distributes smoothly and decreases from inlet to exit. And at impeller exit, the relative velocity is lower close to suction side than that near pressure side of blade in most of blade channels. This flow structure is somewhat of jet-wake flow structure in centrifugal impeller. It is because the blade exit angle is 39°, greater than that of conventional centrifugal pump. There are some differences in flow patterns between different blade channels. The relative velocity in the blade channel close to pump exit is higher than that in other channels. The relative streamlines in blade channel distribute along the blade surface smoothly and there is no circulation in the channel under this condition.
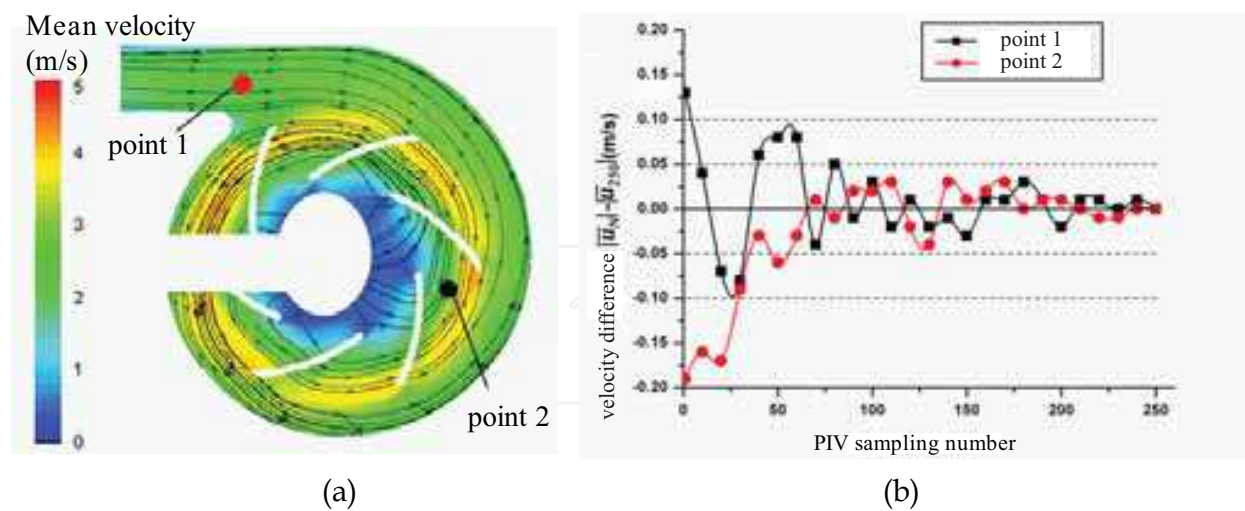
Fig. 3. The distributions of sampling points (a) and measuring uncertainty (b) at design follow rate condition
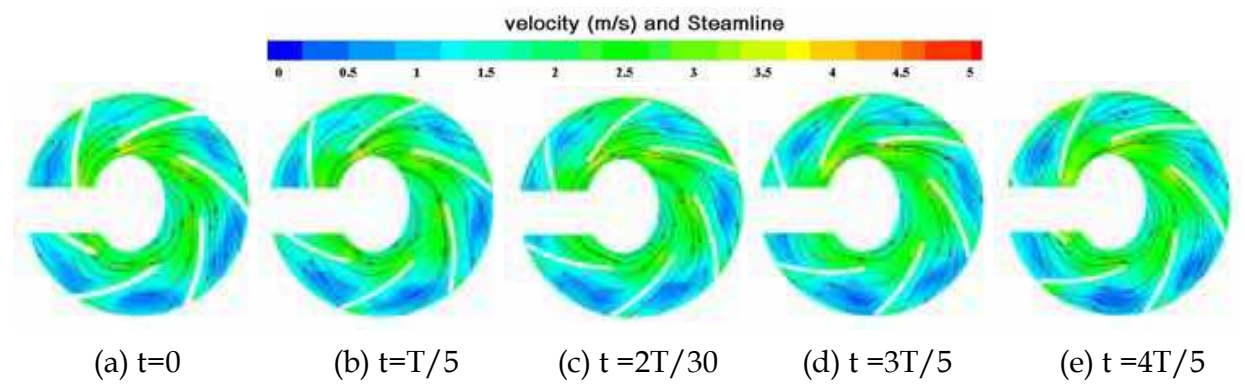

(a) t=0   (b) t=T/5   (c) t =2T/30   (d) t =3T/5   (e) t =4T/5

Fig. 4. Relative velocity and streamlines in impeller at design flow rate condition ($Q=Q_d$)

4.3 Absolute velocity distribution and streamlines in volute at design flow rate

Fig. 5 shows the absolute velocity and streamlines in volute at design flow rate condition. The flow distributions on 5 pictures of volute at different moments are almost the same that are smooth and almost even. The absolute velocity is higher than that in other position near the tongue. So the flow pattern in the pump volute is stable under the desin flow rate condition.

(a) t=0   (b) t=T/5   (c) t =2T/30   (d) t =3T/5   (e) t =4T/55
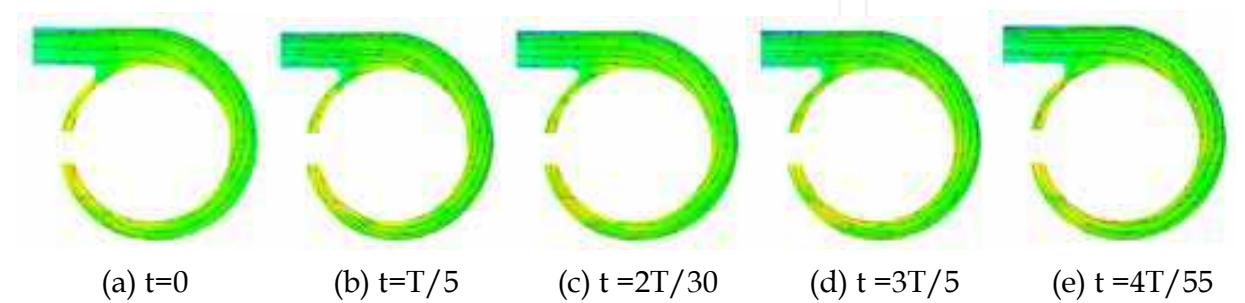
Fig. 5. The absolute velocity and streamlines in volute at design flow rate condition ($Q=Q_d$)

5. Computational results and dissicusion

5.1 Pump energy performances' prediction

Table 3 and Fig. 6 show the steady and unsteady calclated and tested energy performances of the centrifugal pump in 8 different flow rate cases. The calculated energy performances are predicted with distributions of velocity and pressure obtained through either steady flow simulation or unsteady flow simulation in the computational domain.

flow rate	tested head	tested efficiency	Steadty calculated head	steady calculated efficiency	unsteady calculated head	unsteadtycalculated efficiency
$Q(\text{m}^3/\text{h})$	$H_{\text{exp}}(\text{m})$	$\eta_{\text{exp}}(\%)$	H_{ss} (m)	$\eta_{\text{ss}}(\%)$	$H_{\text{us}}(\text{m})$	$\eta_{\text{us}}(\%)$
0.85	1.4879	31.40	1.5538	30.62	1.5316	30.02
1.00	1.4883	34.10	1.5354	34.85	1.5226	34.11
1.41	1.4859	42.14	1.4934	40.50	1.4760	40.01
2.00	1.4578	47.89	1.4363	45.92	1.4498	46.04
2.41	1.4196	51.02	1.3724	46.59	1.4224	51.12
2.70	1.3912	52.40	1.3889	58.03	1.4007	54.67
2.98	1.3466	52.86	1.3524	57.71	1.3785	55.15
3.36	1.3006	51.16	1.2467	53.62	1.3209	52.27

Table 3. Calclated and tested energy performances of the centrifugal pump
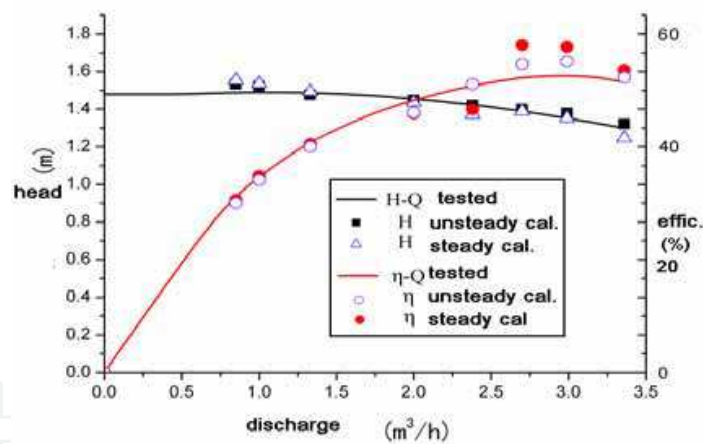
Fig. 6. Calclated and tested energy performances of the centrifugal pump

Fig. 6 shows that predicted pump energy performances both in steay and unsteady flow computations agree with test data. The calculated head of the pump is larger than tested one in small flow rate cases and smaller in large flow rate cases. But errors between calculated head and tested one are less than 5%. The predicted efficiency is closed to the test one in design and small flow rate cases, and higher than the tested one in large flow rate cases. As a whole, the predicted performance data in unsteady flow simulatiom are closer to test data than thoses in steady flow simulation.

5.2 Internal flow patterns verification

In order to verify the reliability of CFD results, it is necessary to compare computational and PIV measured flow velocity distributions both in the pump impeller and in its volute.

Steady numerical simulation method

Fig. 7 show relative velocity distributions and streamlines in impeller in design flow case both in CFD steady flow simulation (a) at the frozen position of impeller for t = 0 moment and in PIV measurement at this position. The PIV data are the averaged results of 200 times of measurement. Fig. 8 is absolute velocity and streamlines in volute in design flow case obtained through the same computation and measurement as those in Fig. 5.
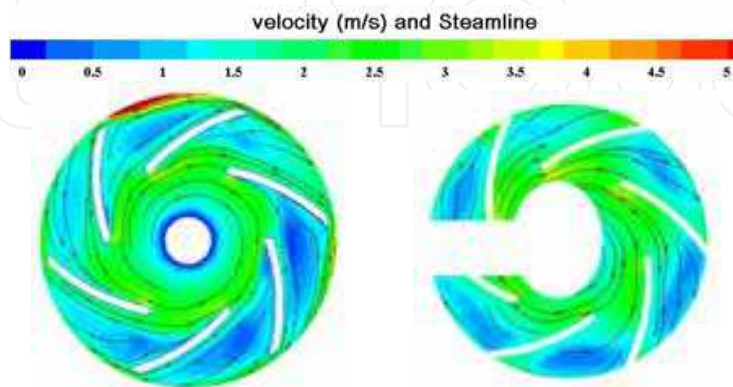
(a) Velocity by steady flow simulation (b) PIV measured velocity

Fig. 7. Relative velocity and streamlines in impeller at design flow rate case (Q=Q$_d$)
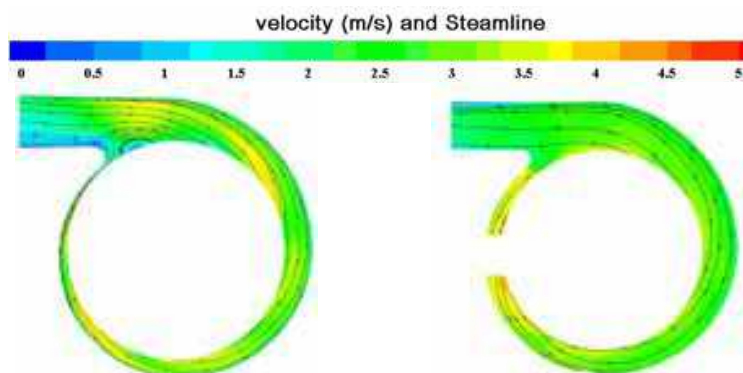
(a) Velocity by steady flow simulation (b) PIV measured velocity

Fig. 8. Absolute velocity and streamlines in volute at design flow rate case (Q=Q$_d$)

Comparison of tested results at t = 0 moment of PIV measurement shows that the relative velocity in CFD steady flow simulation in the impeller is larger than that of test data under design flow rate condition (see Fig. 7). In the volute, there is a circulation area at its outlet in steady flow simulation (shown in Fig. 8), but there is no such circulation in Fig. 8 (b) of PIV results. And the simulated absolute velocity values by CFD at the volute outlet section varies greatly.

Verification of velocity distributionsof of unsteady flow computation

Fig. 9 show relative velocity distributions and streamlines in impeller in design flow case in CFD unsteady flow simulation at its positions selected for (a) t=0, (b) t=T/5, (c) t=2T/5 (d) t =3T/5 and (e) t =4T/5 moments. And Fig. 4 displays the same results by in PIV intantiniors measurement as thoses in Fig. 9. Fig. 10 and Fig. 5 are absolute velocity distributions and

streamlines in volute in design flow case obtained through the same unsteady flow computation and measurement.
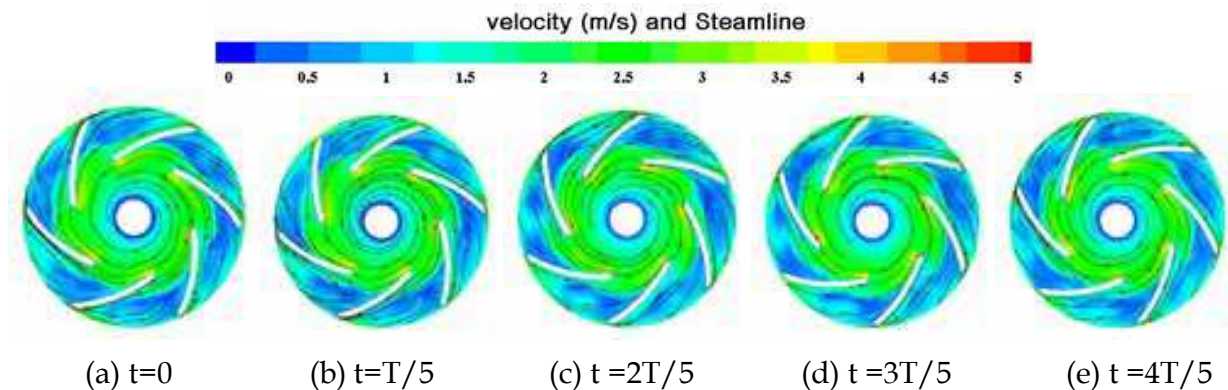

| (a) t=0 | (b) t=T/5 | (c) t =2T/5 | (d) t =3T/5 | (e) t =4T/5 |

Fig. 9. Computed relative velocity and streamlines in impeller at design flow rate ($Q=Q_d$)
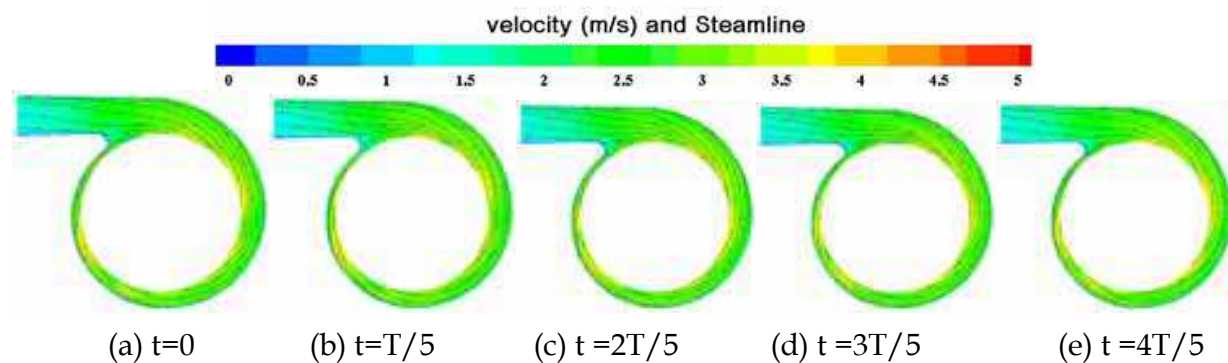

| (a) t=0 | (b) t=T/5 | (c) t =2T/5 | (d) t =3T/5 | (e) t =4T/5 |

Fig. 10. Computed absolute velocity and streamlines in volute at design flow rate ($Q=Q_d$)

Under this design fow rate condition, the numerical results of unsteady flow computation agree with PIV instantaneous mesurement data, which indicates the unsteady turbulent flow simulation in the centrifugal pump is successful and reliablel.

5.3 Steady flow simulation results

Fig. 11 (a) to (c) are the steady flow calculation results of relative velocity and streamlines in the pump impeller at t=0 moment in small flow rate case, $Q=52\%Q_d$, in design flow rate case, $Q=Q_d$, and in large flow rate case, $Q=124\%Q_d$, respectively. Fig. 13 (a) to (c) are the steady flow calculation results of absolute velocity and streamlines in the volute at t=0 moment in the three flow rate cases. The coresponding PIV tested results are showm in Fig. 12 and Fig. 14.

In Fig. 11 and Fig. 12, it is shown that under the small flow rate condition, the vortex positions in pump impeller of calculated results do not agree with the test data, and the distribution of relative velocites are different with each other. Under the design condition and the large flow rate condition, the numerical predicted relative velocity magnitutes are larger than those obtained from PIV measurement (shown in Fig. 12). There are some vortecies in the pump volute in the three flow rate cases from the calculated results in Fig. 13, but those vortecies do not appear in PIV test results in Fig. 14.

The predicted performances in staedy flow simulation agree with the test data very well (shown in Fig. 6). But there are some differences of velocities both in the pump impeller and
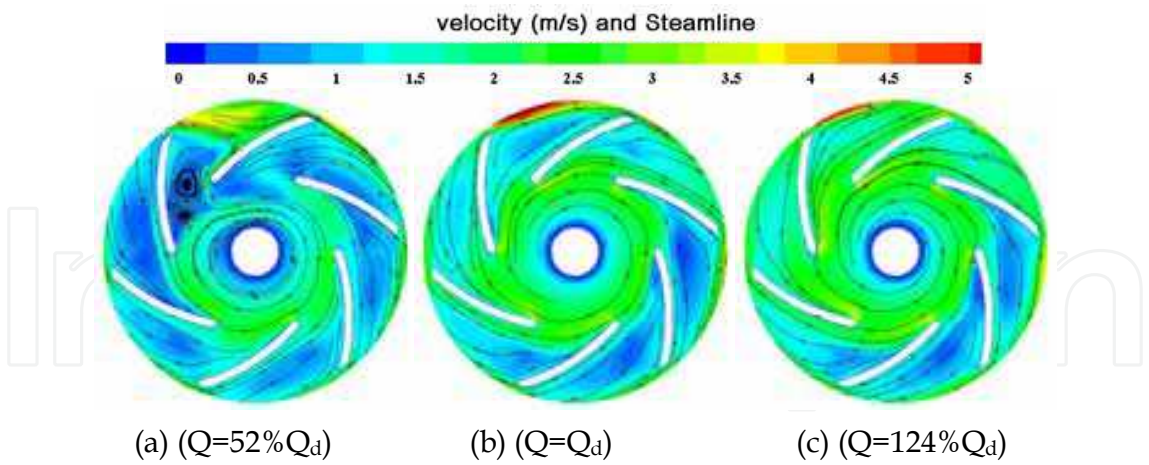
(a) (Q=52%Q$_d$)   (b) (Q=Q$_d$)   (c) (Q=124%Q$_d$)

Fig. 11. Steady flow calculation results of relative velocity and streamlines in impeller at t=0
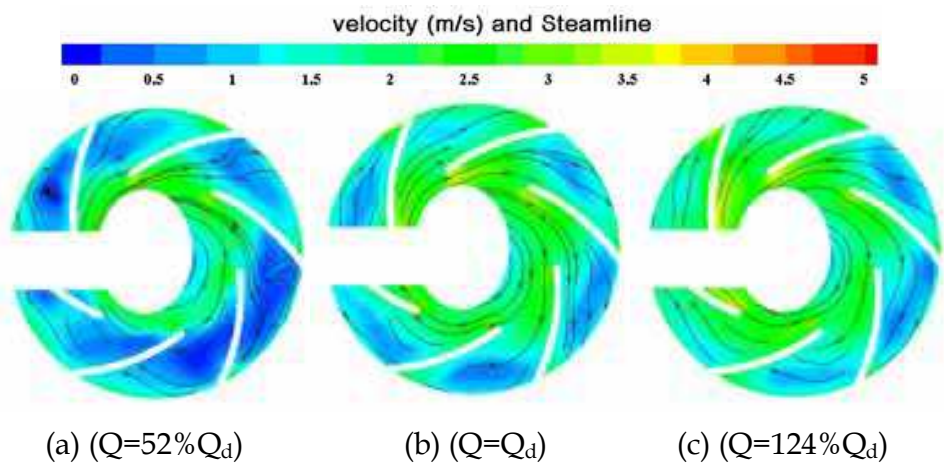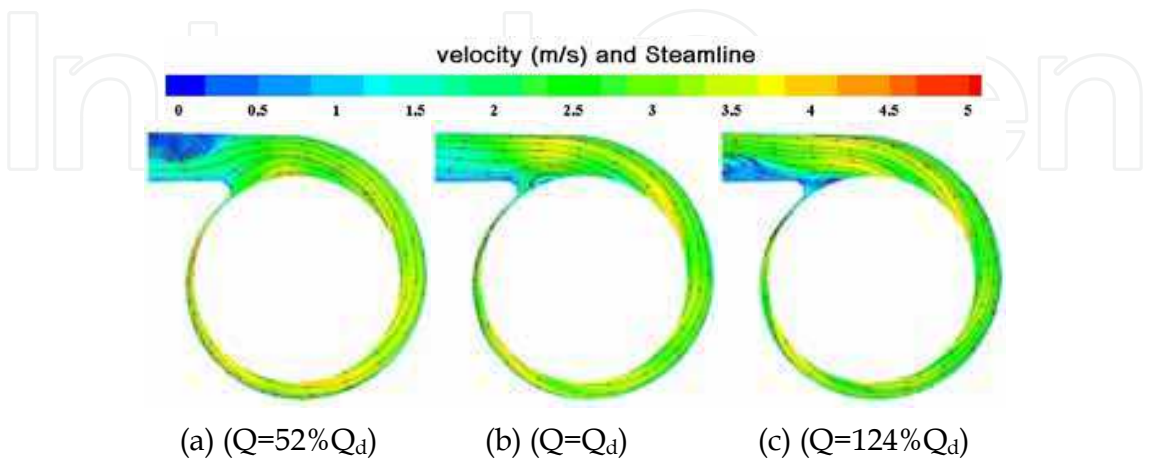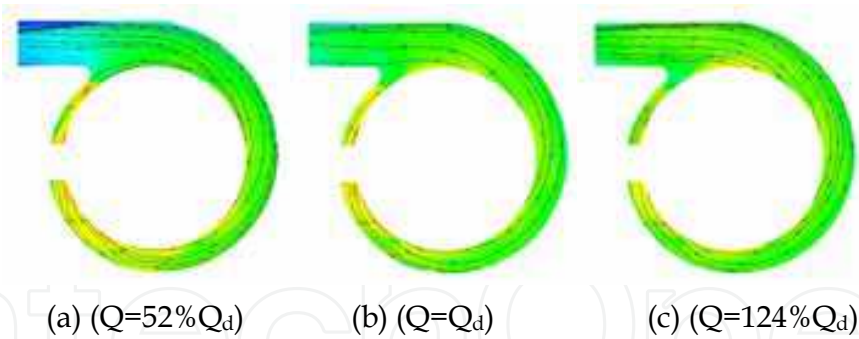(a) At small flow rate case (b) At design flow rate case (c) At large flow rate case

(a) (Q=52%Q$_d$)   (b) (Q=Q$_d$)   (c) (Q=124%Q$_d$)

Fig. 12. PIV tested results of relative velocity and streamlines in impeller at t=0
(a) At small flow rate case (b) At design flow rate case (c) At large flow rate case

(a) (Q=52%Q$_d$)   (b) (Q=Q$_d$)   (c) (Q=124%Q$_d$)

Fig. 13. Steady flow calculation results of absolute velocity and streamlines in volute at t=0
(a) At small flow rate case (b) At design flow rate case (c) At large flow rate case

(a) (Q=52%Q_d)   (b) (Q=Q_d)   (c) (Q=124%Q_d)

Fig. 14. PIV tested results of absolute velocity and streamlines in volute at t=0
(a)At small flow rate case (b) At design flow rate case (c) At large flow rate case

the pump volute between steady flow simulation and PIV measurement. The steady flow simulation is based on the frozen model, that is, the fixed position of impeller blades in this computation. But in reality, the baldes are rotating, and that is not simulated in the steady flow calculation.

5.4 Unsteady flow simulation results at off-design flow rate conditions

Fig. 15 and Fig. 16 show the unsteady flow calculation results of relative velocity and streamlines in the pump impeller in small flow rate case, Q=52%Q_d, and in large flow rate case, Q=124%Q_d, respectively, at different moments. Fig. 17 and Fig. 18 indicate the unsteady flow calculation results of absolute velocity and streamlines in the pump volute in the two off- design flow rate cases, respectively.

t=0   t=T/5   t=2T/5   t=3T/5   t=4T/5
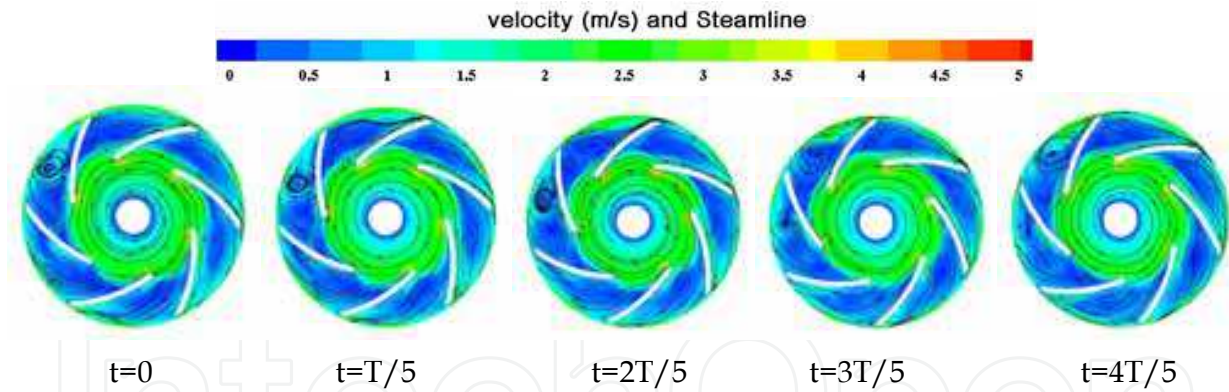
Fig. 15. Unsteady flow calculation results of relative velocity and streamlines in impeller at the small flow rate case (Q=52%Q_d)

From Fig. 15, it is obvious that under the small flow rate condition, there are some vortexies in the pump impeller according to the unsteady flow simulation, and their magnitutes are the basically the same as those in the PIV instantaneous measurement (see Fig. 12 (a)). The absolute velocities and streamlines distributions in the pump volute agree well between the unsteady flow simulation in Fig. 17 and PIV instantaneous measurement in the small flow rate case (see Fig. 14 (a)). But under the large flow rate condition, the agreement between them is worse than that under small flow rate condition (see (see Figs. 12 (c) and 14(c)).
All the comparisons between unsteady flow simulation and the PIV instataneous meausrement indicate that the model and method of the simutation in this work are reliable for prediction of the centrifugal pump internal flow.
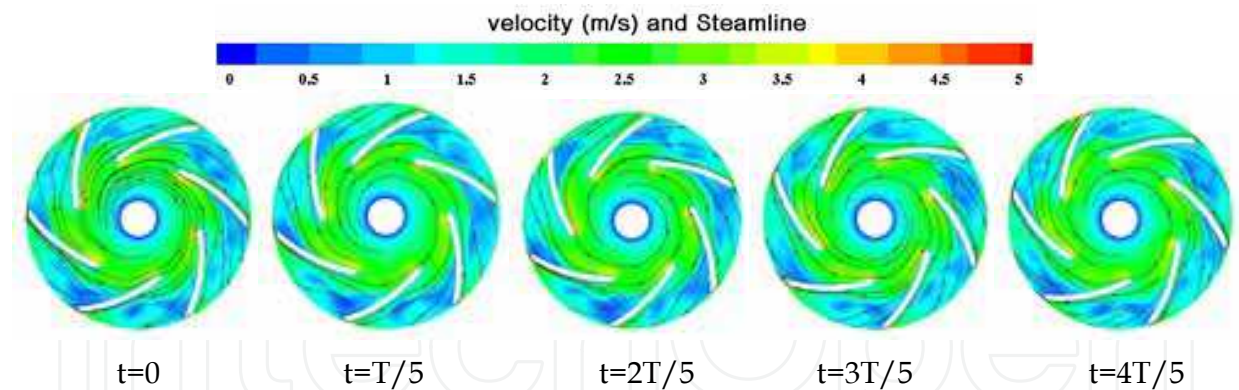
Fig. 16. Unsteady flow calculation results of relative velocity and streamlines in impeller at the large flow rate case (Q=124%Q_d)
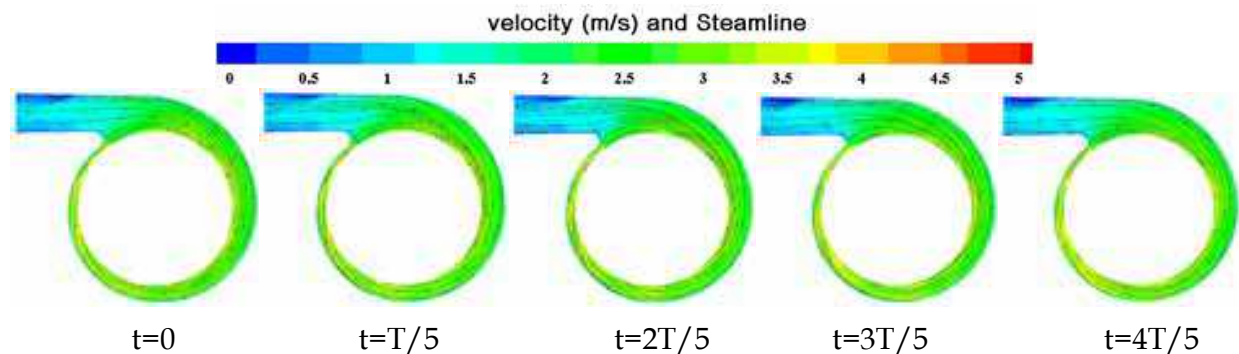

Fig. 17. Unsteady flow calculation results of absolute velocity and streamlines in volute at the small flow rate case (Q=52%Q_d)
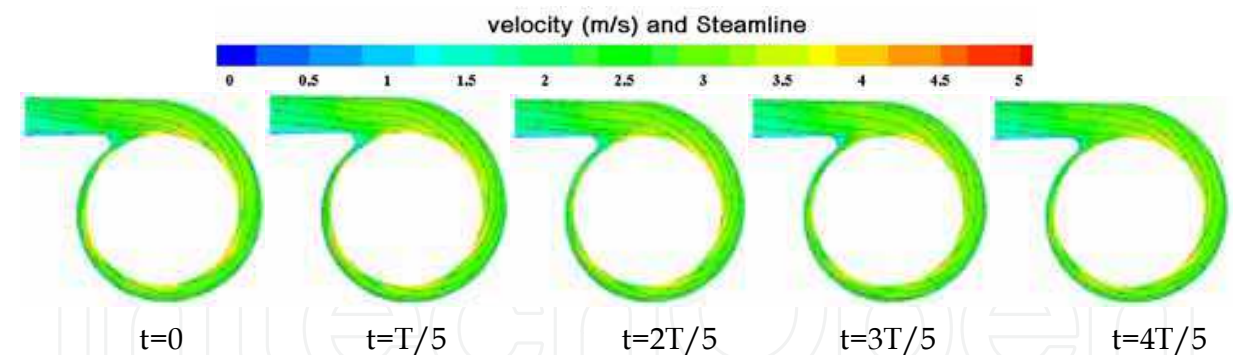

Fig. 18. Unsteady flow calculation results of absolute velocity and streamlines in volute at the large flow rate case (Q=124%Q_d)

6. Conclusion

The RANS tubulent equations with the SST k-ω turbulence model are applied to simulate the 3D steady whole passage flow in a centrifugal pump and the DES method based on the SST k-ω turbulence model to simulate this unsteady flow. The external characteristics and the internal flow pattern of the centrifugal pump are calculated. From the computational results compared with the pump peformance test and its PIV measurement the following conclusions could be drawn:

1. The calculated energy performances can be predicted through distributions of velocity and pressure obtained in either steady flow simulation or unsteady flow simulation in the pump computational domain. The predicted performance data in unsteady flow simulatiom are closer to test data than thoses in steady flow simulation.
2. Comparison between tested results at t=0 moment of PIV measurement and calculated ones, the velocity distribution in CFD steady flow simulation both in pump impeller and volute is larger than those of test data under design flow rate condition.
3. Under design fow rate condition, the numerical results of unsteady flow computation agree with PIV instantaneous mesurement data, which indicates the unsteady turbulent flow simulation in the centrifugal pump is reliable.
4. The unsteady flow simulation in the pump are also carried out under off-design conditions. The velocities and streamlines distributions agree well between the unsteady flow simulation and PIV instantaneous measurement in the small flow rate case. But under the large flow rate condition, the agreement between them has more tolerance than that under small flow rate condition.

7. References

Budwig, R. (1994). Refractive index matching methods for liquid flow investigations, *Experiments in Fluids*, Vol.17, (Oct. 1994) 350-355, ISSN 0723-4864

Burgreen, G.W.; Antaki, J.F. & Griffith, B.P. (1996). A design improvement strategy for axial blood pumps using computational fluid dynamics, *ASAIO J.*, Vol. 24, No. 5, (Sept. 1996) M354-M360, ISSN 10582916

Burgreen, G.W.; Antaki, J.F.; Wu, J. & Holmes, A. J. (2000). CFD-based design optimization of the UoP streamliner rotary blood pump, *Proc. 2000 Annual Fall Meeting of the Biomedical Engr. Society, Washington*, Oct. 2000, ISBN: 00906964, Am Inst Phys, Woodbury, NY

Byskov, R.K.; Jacobsen, C.B. & Pedersen, N. (2003a). Flow in a centrifugal pump impeller at design and off-design conditions—Part II: Large Eddy Simulations, *J. Fluids Eng.*, Vol. 125, No. 1, (Jan. 2003) 73-82, ISBN 00982202

Feng, J.; Benra, F.K. & Dohmen, H.J. (2009). Comparison of periodic flow fields in a radial pump among CFD, PIV, and LDV results, *Inter. J. of Rotating Machinery*, Vol. 2009. Article ID 410838, 10 pages, ISBN 1023621X

Guleren, K.M. & Pinarbasi, A. (2004). Numerical simulation of the stalled flow within a vaned centrifugal pump, *Proc Instn Mech. Engrs, J. Mechanical Engineering Science*, Vol. 218, Part C, (Apr. 2004) 425-435, ISBN 09544062

Li, J.W.; Liu, S.H.; Luo, X.W. & Wu, Y.L. (2007). Viscous flow field in a mini pump with an asymmetric axis, *J. Tsinghua Univ. (Sci & Tech)*, Vol 47, No.5, (May 2007) 682-685, ISSN 10000054

Matsui, J.; Choi, Y.D.; Kurokawa, J.; Imamura, H. & Hara, M. (2002). Internal flow in a centrifugal pump of a low specific speed with semi-open impeller, *Tran. of the JSME, Part B*, Vol. 6, No. 668, (Apr. 2002) 1174-1180, ISSN 03875016

Menter, F. R. (1994). Two-equation eddy-viscosity turbulence models for engineering applications. *AIAA Journal*, Vol. 32, No. 1, (Jan. 1994) pp: 269-289, ISBN: 00011452

Mitchell, A.M.; Morton, S.A.; Forsythe, J. R. & Cummings, R.M. (2006). Analysis of delta-wing vortical substructures using detached-eddy simulation. *AIAA Journal*, Vol. 44, No. 5, (May 2006) 964-972, ISSN 0001452

Pedersen, N. & Larsen, P.S. (2003b). Flow in a centrifugal pump impeller at design and off-design conditions—Part I: Particle image velocimetry (PIV) and laser doppler velocimetry (LDV) measurements, *J. Fluids Eng.* , Vol. 125, No. 1, (Jan. 2003) 61-72, ISBN 00982202

Song X.; Wood H., G.; Day S. W. & Olsen D. D. (2003). Studies of turbulence models in a CFD model of a blood pump, *Artificial Organs*, Vol. 27, No. 10, (2003 Oct.) 938-941, ISBN: 0160-564X

Wu, Y.L., Yuan, H.J., Shao, J. & Liu, S.H. (Apr. 2009). Experimental study on internal flow of a mini centrifugal pump by PIV measurement. Inter. J. of Fluid Machinery, Vol. 2, No. 2, (Feb. 2009), 121-126, ISSN 1882-9554
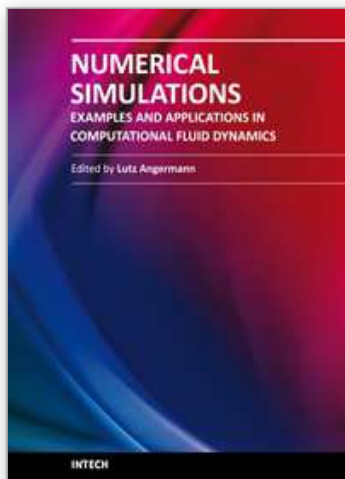
Numerical Simulations - Examples and Applications in Computational Fluid Dynamics
Edited by Prof. Lutz Angermann

This book will interest researchers, scientists, engineers and graduate students in many disciplines, who make use of mathematical modeling and computer simulation. Although it represents only a small sample of the research activity on numerical simulations, the book will certainly serve as a valuable tool for researchers interested in getting involved in this multidisciplinary ï¬eld. It will be useful to encourage further experimental and theoretical researches in the above mentioned areas of numerical simulation.

How to reference
In order to correctly reference this scholarly work, feel free to copy and paste the following:

Wu Yulin, Liu Shuhong and Shao Jie (2010). Numerical Simulation on the Steady and Unsteady Internal Flows of a Centrifugal Pump, Numerical Simulations - Examples and Applications in Computational Fluid Dynamics, Prof. Lutz Angermann (Ed.), ISBN: 978-953-307-153-4, InTech, Available from:
http://www.intechopen.com/books/numerical-simulations-examples-and-applications-in-computational-fluid-dynamics/numerical-simulation-on-the-steady-and-unsteady-internal-flows-of-a-centrifugal-pump

INTECH
open science | open minds